JOURNAL OF MATERIALS SCIENCE 15 (1980) 2207–2220

The hydrostatic extrusion of polymethylmethacrylate

P. S. HOPE, I. M. WARD
Department of Physics, University of Leeds, Leeds, UK
A. G. GIBSON
Department of Metallurgy and Materials Science, University of Liverpool, Liverpool, UK

The hydrostatic extrusion behaviour of two grades of polymethylmethacrylate (PMMA) is reported and an analysis of the mechanics of the extrusion process is presented. Although the maximum degree of deformation achieved is considerably lower than that obtained for crystalline polymers, the process mechanics are controlled by the same factors (i.e. the billet-die friction, and the effects of strain rate and pressure on the material flow stress). A method for equating the effects of pressure and friction is described, following the work of Tabor on the adhesive mechanism of friction in polymers. This method gives a friction coefficient in the range 0.1 to 0.2 for the hydrostatic extrusion of PMMA, compared to values in the region 0.03 to 0.08 for crystalline polymers, suggesting conditions of boundary lubrication. The relatively high values of friction for PMMA are consistent with the requirement for careful preparation of the billet surface prior to extrusion, and the observation of the "stick–slip" phenomenon during extrusion. The differences between the grades of PMMA in both extrusion behaviour and tensile drawing behaviour are explicable in terms of their different glass transition temperatures.

1. Introduction

Solid state extrusion of polymers has been of interest in the study of crystalline polymers, where it has been possible to produce highly oriented structures in quite substantial cross sections for engineering and scientific studies [1–10]. Moreover the hydrostatic extrusion process, being close to an ideal tensile deformation, has proved a useful technique for the production of oriented polymers in larger cross section than is achievable by tensile drawing techniques, enabling measurements of transverse modulus [11] and thermal conductivity [12] to be performed.

Although hydrostatic extrusion has been confined primarily to crystalline materials, some preliminary studies have been performed with moderate success on polyvinyl chloride [13], polysulphone [14], polyimide [14] and polymethylmethacrylate (PMMA) [15]. The technique has also been used recently at Leeds University to prepare samples for orientation studies in PMMA and polycarbonate [16].

In general, only a few experimental studies have attempted to link the solid state extrusion behaviour to the plastic flow behaviour of the polymeric material in question, although the understanding of this mechanistic link is well advanced in the metals field [17, 18]. Takayanagi and co-workers [19–21] applied various approaches based on conventional metal-working theory to the ram extrusion of linear polyethylene (LPE), polypropylene and nylon 6. More recently, Gibson, Coates and Ward [22, 23] have applied a modified form of Hoffman and Sachs' lower bound analysis to the hydrostatic extrusion of the crystalline polymers LPE and polyoxymethylene (POM). This latter work showed that for a realistic understanding of process behaviour it was necessary to take

0022–2461/80/09 2207–14$03.40/0

TABLE I Physical characteristics of PMMA grades used in the investigation.

Grade	Type	$\bar{M}_w$*	T_g(°C)†
A	homopolymer	2,000,000	110
B	copolymer	250,000	104

*Manufacturers data

†Measured by differential scanning calorimetry at a heating rate of 10° C min^{-1}.

into account not only die friction and strain hardening, but also strain rate and pressure dependence of the material flow stress.

Our earlier studies of the hydrostatic extrusion of crystalline polymers have highlighted the marked effect of molecular weight and copolymerization on processing behaviour [6, 9, 10]. The purpose of the present work was to determine the range of deformation ratios which could be achieved using two grades of PMMA, different from each other in both molecular weight and type. Grade A (see Table I) is a high molecular weight homopolymer produced by monomer casting, while grade B is a lower molecular weight copolymer, normally used for injection moulding. Nevertheless, it has been shown previously that the tensile drawing behaviour of PMMA is not determined in the first order by molecular weight, but rather by the free monomer content of the samples used [24]; this in turn correlates with the glass transition temperature (T_g) of the polymer. It was therefore expected that the difference in T_g between the grades investigated would result in different true stress–strain–strain rate behaviour, which would be reflected by differences in the observed hydrostatic extrusion behaviour.

Another major effect, the "stick–slip" phenomenon, first determined for hydrostatic extrusion of metals [25], has proved a major difficulty in the solid state processing of polymers. This instability has been discussed qualitatively for the case of polymers [6, 8, 9], and it has been outlined that pressure dependence, frictional behaviour and deformational heating all play a part in accentuating the effect in the case of the latter materials. It is probably true that insufficient weight has been given to the importance of "stick–slip" in experimental accounts of the hydrostatic extrusion of polymers.

In our previous studies of crystalline polymers the limiting deformation behaviour at higher deformation ratios was attributed to a combination of friction and pressure dependence effects, but these effects were not satisfactorily separated. In the present study of PMMA we found frictional effects to be particularly important, both in determining process instabilities ("stick–slip") and in steady state process behaviour. This is partly due to the fact that the friction coefficient of PMMA is much higher than that of the previously studied LPE and POM, and also because the extrusion behaviour is particularly sensitive to the surface condition of the material. In examining this effect we have drawn from recent work by Tabor and coworkers on frictional behaviour, and this has led to a useful rationalization of both friction and pressure effects.

2. Sample preparation

Details of the two molecular weight grades investigated are shown in Table I. Grade A was supplied in the form of cast rod, while grade B was supplied in bead form, from which rods were produced by injection moulding at 240° C into a heated cylindrical mould. A mould temperature of 115° C was used, as bulk flow lines were visible in mouldings produced at mould temperatures below T_g. All mouldings were allowed to cool for about 5 minutes until the temperature had fallen to below T_g, when they could be pressed out of the mould. Billets for extrusion were machined from these rods and were cylindrical, with a 15° semi-angle nose cone to facilitate an initial pressure seal in the extrusion die.

Test specimens for tensile true stress–strain–strain rate measurements were routed from cast sheet in the case of grade A, and from compression moulded sheets in the case of grade B. The samples were polished prior to testing in order to remove surface defects introduced by the machining operation.

3. Hydrostatic extrusion experiments

3.1. Equipment

The hydrostatic extrusion apparatus, which has been described in detail in previous publications [6, 9], consisted of a heated extrusion vessel and separate ram intensifier, driven by a conventional hydraulic circuit. A pressure relief valve in the primary circuit was used to control the extrusion vessel pressure (P), which was measured by means of a strain-gauge pressure transducer. The pressure transmitting fluid was castor oil.

A conical extrusion die with an exit-bore diameter (d_f) of 7 mm and semi-angle (α) of 15° was

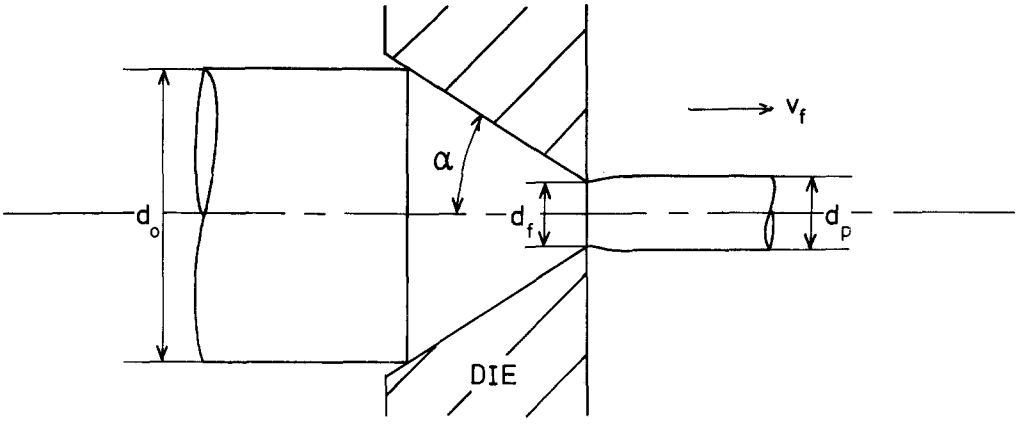

$$\text{Nominal extrusion ratio} \quad R_N = \frac{\text{Area of cross-section of billet}}{\text{Area of cross-section of die exit}} = \left(\frac{d_o}{d_f}\right)^2$$

$$\text{Actual extrusion ratio} \quad R_A = \frac{\text{Area of cross-section of billet}}{\text{Area of cross-section of product}} = \left(\frac{d_o}{d_p}\right)^2$$

Figure 1 Main process variables in hydrostatic extrusion.

used throughout the investigation. During extrusion the extrudate velocity (v_f) was monitored using a potentiometer, driven via a light-weight haul-off system attached to the extrudate. Because the product swelled on leaving the die it was necessary to define an actual extrusion ratio, related to the product cross-sectional area, as well as a nominal extrusion ratio based on the die exit area (see Fig. 1).

3.2. Procedure

For all extrusions the billets were loaded into the pre-heated extrusion vessel and left for at least one hour to achieve thermal equilibrium at the desired extrusion temperature (T_N). The pressure was then raised in steps until extrusion commenced.

During initial experiments the phenomenon of "stick–slip" was observed, in which the product emerged from the die in a series of jerks while the extrusion pressure oscillated. The extrudate produced from such extrusions contained many surface cracks and was frequently distorted, as shown in Fig. 2a. Such "stick–slip" behaviour has been observed previously in the extrusion of metals [25] and some other polymers [6, 8, 9, 16], and may be attributed in the case of metals to the difference between the static and non-static coefficients of friction at the billet-die interface. For polymers the phenomenon may be aggravated by two additional effects; the pressure dependence of the flow stress of the material, and the occurrence of adiabatic heating, both of which reduce the extrusion pressure once extrusion has commenced. One way to reduce the effect of "stick–slip" is to minimize the elastic stored energy in the extrusion fluid, which may be achieved by the use of steel coring to reduce the fluid volume. Another method, used successfully in metals extrusion, is reduction of the initial billet-die friction by sand-blasting the surface of the billet. Both methods were subsequently used in PMMA extrusions, and were found to reduce the severity of the "stick–slip" behaviour. In particular, sand-blasting al-

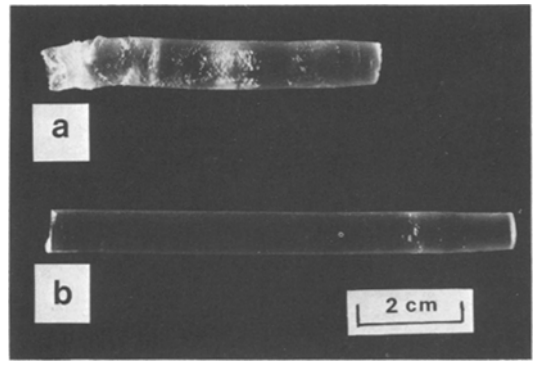

Figure 2 PMMA extrudates (a) distorted, showing surface cracking (b) undistorted.

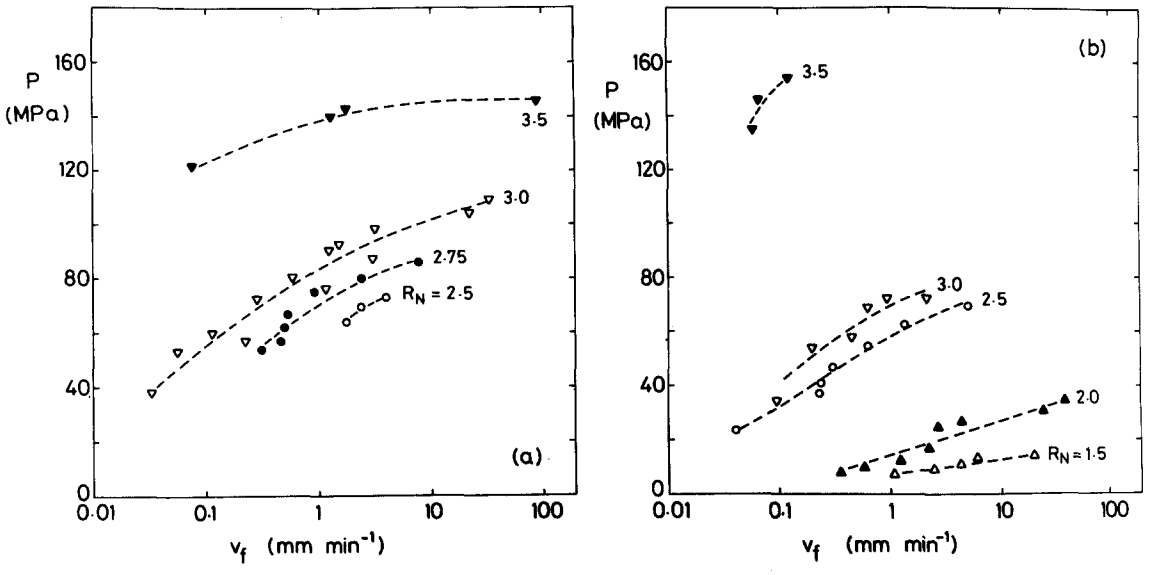

Figure 3 Variation of extrusion pressures with extrudate velocity (T_N = 90° C) (a) Grade A (b) Grade B

lowed stable extrusions to take place at extrusion ratios far in excess of those obtained using smooth billets.

Throughout the series of extrusions brittle fracture of the extrudate commonly occurred at the die exit, even when no haul-off force was applied. The incidence of this type of failure was reduced by polishing the surface of the billet prior to extrusion, which removed surface cracks introduced during the machining operation. Subsequent sand-blasting to reduce the severity of the "stick–slip" behaviour did not appear to undo the beneficial effects of polishing. This was attributed to a difference in the nature of the cracks introduced by sand-blasting, which were smaller and less localized than those introduced during machining.

Much of the surface cracking and many of the extrudate fractures were reminiscent of stress cracking failures observed in the hydrostatic extrusion of LPE [6, 9]. Environmental stress cracking occurs at the entrance to the die zone, where the material undergoes a tensile stress while in contact with the extrusion fluid, giving rise to surface micro-cracking on the extrudate. If severe, this may lead to instability and fracture at the die exit. As the severity of the attack depends on the time for which the stress acts, it was possible in the case of LPE to eliminate the problem completely by extruding at sufficiently high rates. Unfortunately such high rates were not achieved in the case of PMMA, and so an alternative method was used, namely coating the billets with a latex rubber prior to extrusion. This procedure has been used by Harris *et al.* [26] to prevent premature fracture during torsional tests on PMMA under hydrostatic pressure. Before loading into the extrusion apparatus the entire billet was dipped in a latex suspension, which was allowed to dry before curing in air. The protective coating was found to remain intact until extrusion commenced, whereupon the film ruptured in the die. Nevertheless, stress cracking attack could be avoided by this method at all but the slowest production rates.

The best results were therefore obtained by adopting the following procedure for billet preparation; (i) Polish billet surface; (ii) Sand-blast billet surface; (iii) Coat billet surface with latex rubber.

Use of the above procedure allowed controlled, steady state extrusions to be performed in both grades of PMMA. Although in some cases (notably at higher extrusion ratios) products of the type shown in Fig. 2a were still obtained, the products were mostly clear and unblemished, as shown in Fig. 2b. It is notable that use of the same procedure greatly improved the hydrostatic extrusion behaviour of another amorphous glassy polymer, polycarbonate, which is currently being investigated in our laboratory [16].

3.3. Results

In early experiments in our laboratories Kahar [15] performed extrusions at velocities in the region of 1 mm min^{-1}, using grade A at extrusion temperatures of 50° C and 90° C. This work was extended by the present authors to higher ex-

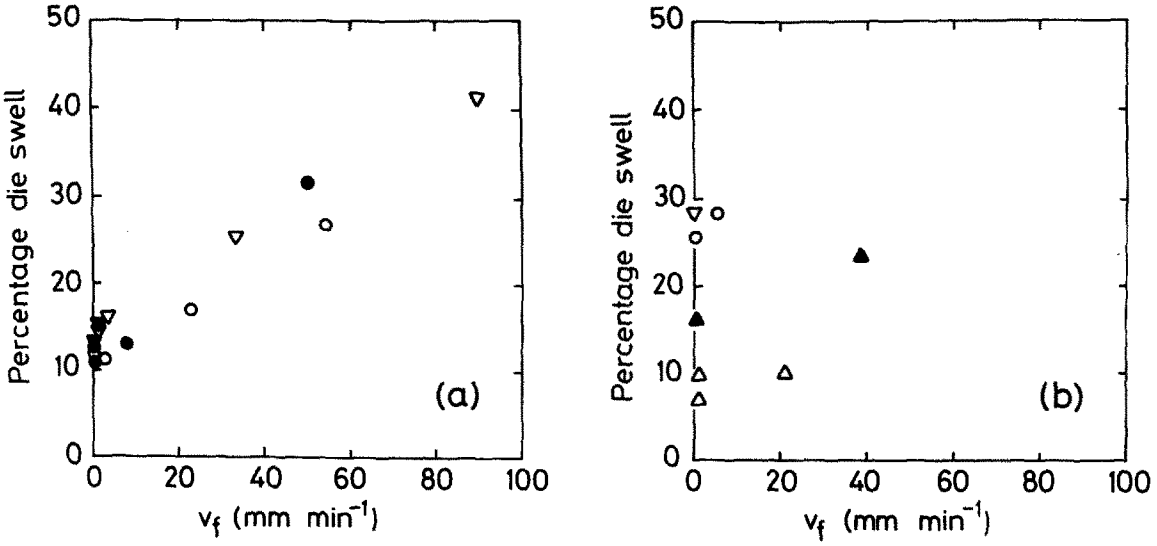

Figure 4 Variation of die-swell with extrudate velocity ($T_N = 90°$ C); $R_N = 1.5$ △; 2.0 ▲; 2.5 ○; 2.75 ●; 3.0 ▽; 3.5 ▼ (a) Grade A (b) Grade b

trusion ratios for grade A at 90° C, and a comparable set of extrusions was performed using grade B, also at 90° C. The effect of extrusion velocity was investigated for both grades.

The variation of extrusion pressure with extrudate velocity is shown in Fig. 3 for a number of extrusion ratios at $T_N = 90°$ C. The maximum extrusion ratio of $R_N = 3.5$ is the same for both grades, and is very much lower than has been obtained for the extrusion of crystalline polymers [1–10], where extrusion ratios as high as 30 have been reported. The product quality was excellent for grade A up to $R_N = 3.0$, and for grade B up to $R_N = 2.0$, above which product distortion and surface cracking were observed. As the onset of product distortion occurs at a lower extrusion ratio in the lower molecular weight polymer, it may be related to a difference in the environmental stress cracking behaviour between the grades.

Stable extrusion could not be obtained at ratios in excess of $R_N = 3.5$, even by the application of a haul-off stress to the product, which always resulted in fracture at the die exit.

The form of the curves in Fig. 3 is similar for both grades, the required extrusion pressure increasing monotonically with both extrusion ratio and extrudate velocity. However, unlike previously reported results for the extrusion of crystalline polymers [6, 7], there is no trace of an upturn in the curves which could lead to a limiting extrusion velocity. Indeed, the extrusion pressure appears instead to be levelling out at higher velocities. This is probably because the effect of strain rate on the material flow stress is much smaller here than for the crystalline polymers, where higher extrusion ratio results are presented. Also, because of the thickness of the extrudates, the possibility of some heat of deformation remaining in the product at higher extrudate velocities, leading to non-isothermal conditions, cannot be ruled out [6, 8, 9].

Large degrees of die-swell were observed in all extrusions. This is shown in Fig. 4, where the percentage die-swell (defined as the fractional increase in product diameter on leaving the die) can be seen to increase linearly with extrudate velocity for grade A, from about 10% at $v_f < 1$ mm min^{-1} to 40% at $v_f = 90$ mm min^{-1}. This linear increase was not seen in grade B extrusions, although the scatter in results is worse and the range of velocities lower than for grade A. Such large degrees of die-swell, which occur as a result of recovery of the elastic deformation, clearly caused the actual extrusion ratios to be considerably lower than the nominal extrusion ratios, particularly at higher production rates.

In Fig. 5, data cross-plotted from Fig. 3 are combined with data from Kahar to give the extrusion pressure–extrusion ratio characteristics at an extrudate velocity of 1 mm min^{-1}. The fact that lower extrusion pressures are required at 90° C than at 50° C for grade A reflects the decrease in flow stress with temperature reported in a previous publication [24]. The even lower extrusion pressures required for grade B imply lower flow stresses than for grade A, provided the other

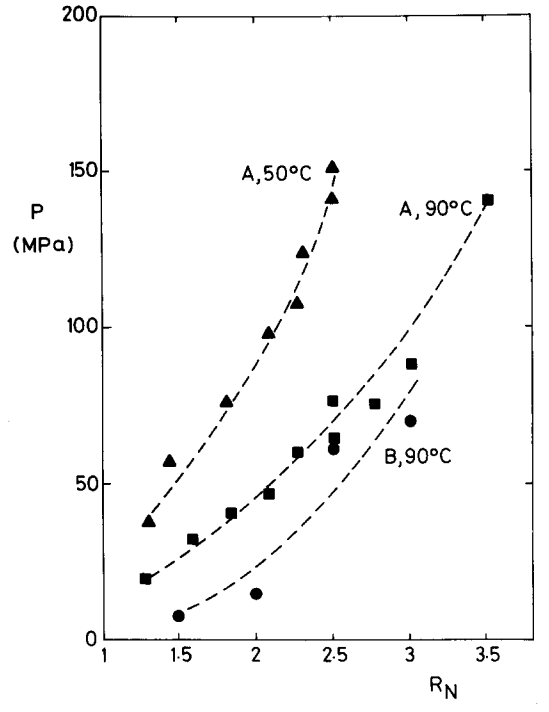

Figure 5 Variation of extrusion pressure with extrusion ratio ($v_f = 1\,mm\,min^{-1}$); triangles, grade A, 50° C; squares, grade A, 90° C; circles, grade B, 90° C.

process parameters remain unaltered. This is investigated in the next section and discussed further in section 5.

4. Flow stress data

It has been argued previously [22, 23] that strain hardening and strain rate effects are very significant in solid state extrusion processes for polymers. It has been shown that a quantitative analysis can be based on appropriate measurements of the tensile drawing behaviour by determining true stress–strain–strain rate curves [27].

In this investigation a modified tensile test at 90° C was used to obtain flow stess data for both grades of PMMA. Such tensile tests are frequently complicated by the formation of a neck, usually accompanied by a load-drop. This behaviour can be understood in terms of the Considère construction [28], which can also be extended to strain rate sensitive materials [29] (at the relevant strain rate). Beyond the load maximum the degree of inhomogeneity of deformation (as well as the size of the load drop) is determined by such factors as (i) Deformational heating; (ii) Hydrostatic component of stress in the neck region; (iii) Strain-softening of the material (i.e. a drop in true stress) if it occurs; (iv) Mechanical testing constraints (gauge length, crosshead speed, load cell compliance etc).

We arranged the test conditions (specimen geometry, crosshead speed) to minimize effects (i) and (ii), so it will be assumed that the main parameters determining neck formation and the magnitude of the load drop were (iii) and (iv).

In some circumstances, it is possible to make the simplifying assumption that the tensile yield behaviour can be represented by a surface in stress–strain–strain rate space. This is equivalent to saying that a constitutive relation exists for the true stress σ in terms of strain ϵ and strain rate $\dot{\epsilon}$ (i.e. $\sigma(\epsilon, \dot{\epsilon})$). We might expect this assumption to hold when the "state" of the material, as represented by its microstructure, depends only on plastic strain, i.e. for crystalline polymers at temperatures below that at which recrystallization or "flow-drawing" occurs, or for amorphous polymers below T_g.

If the above assumption holds, it should be possible to construct the shape of the stesss–strain–strain rate surface from tensile test results over a range of crosshead speeds, despite the fact that results of each individual tests may provide an irregular locus on the σ_f–ϵ–$\dot{\epsilon}$ surface (see for instance refs. 22 and 23).

Specimen geometry and details of the experimental set-up for tensile measurements are shown in Fig. 6. Waisted specimens, 1 mm thick, were used to provide a predictable neck location. Lateral contraction was measured with a linear voltage displacement transducer arranged outside the testing environment to avoid thermal effects. We verified that, for the sample geometry used, lateral and transverse contractions were proportional, enabling the true strain to be measured (assuming constant volume) from the measured change in specimen thickness.

Tensile tests were performed at crosshead speeds of 0.5, 2, 10 and 50 $mm\,min^{-1}$, in order to cover as wide a range of strain rates as possible. Drawing load and contraction in the plane of the sample were recorded during the test using a two-pen recorder. The following procedure was used to determine the relationship between true stress and strain at various constant strain rates:

(1) using the recorded values of contraction, strain versus time plots were constructed for each test;

(2) true stress versus strain curves were

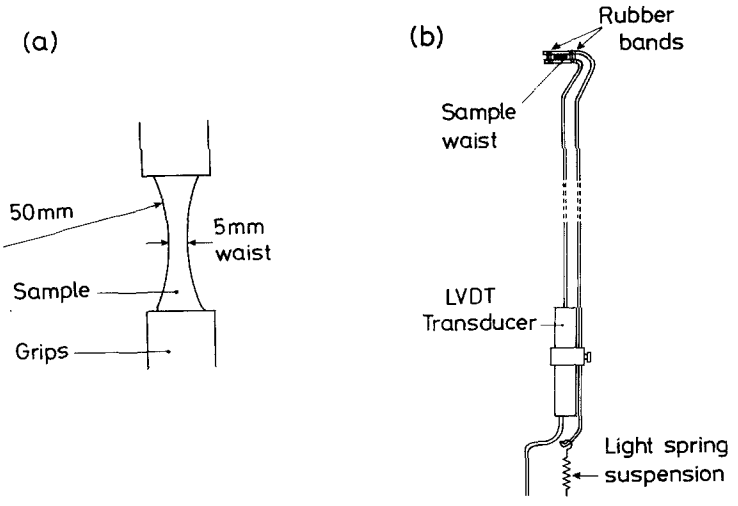

Figure 6 Experimental set-up for tensile measurements (a) Sample and grip geometry (b) Arrangement for measurement of lateral contraction

plotted (for the element of material in the centre of the gauge length) using the load versus time plots and the strain values obtained above;

(3) data from (1) above were further processed (using numerical differentiation) to give plots of $\dot{\epsilon}$ versus ϵ for each test;

(4) graphs of σ_f versus log $\dot{\epsilon}$ were constructed at constant value of strain. Values of σ_f at specific $\dot{\epsilon}$ values were then obtained by interpolation and extrapolation. These were then plotted as true stress–strain curves at constant strain rate. The following strain values were used: 0.02, 0.04, 0.06, 0.08 and 0.1, increasing in steps of 0.1 thereafter.

5. Results and discussion

5.1. The flow stress data

The yield behaviour of polymers differs from that of metals in three major respects

(1) the yield or flow stress is dependent on strain rate;

(2) the flow stress can increase markedly with increasing degrees of plastic strain;

(3) the yield behaviour shows an appreciable dependence on the hydrostatic component of stress.

The simplest representation of the strain rate dependence of the flow stress σ_f is in terms of the Eyring equation [30] so that the strain rate is given by

$$\dot{\epsilon} = \dot{\epsilon}_0 \exp -\left(\frac{\Delta U - \sigma_f V}{KT}\right) \quad (1)$$

where ΔU is the activation energy, V is the activation volume, K is Boltzmann's constant and T is the absolute temperature. This representation suggests that the flow stress at a temperature T is given by

$$\sigma_f = \frac{\Delta U}{Y} + \left(\frac{KT}{V}\right) \ln \left(\frac{\dot{\epsilon}}{\dot{\epsilon}_0}\right) \quad (2)$$

i.e. that the flow stress is a linear function of strain rate.

Fig. 7 shows the true stress versus strain results, plotted at constant grain rate for samples of (a) grade A and (b) grade B. The continuous curves indicate the region within which σ_f values were found by interpolation of experimental data (step 4 above). The range of strain rates covered at each strain level was quite low, of the order of two decades, and there was no sign of significant curvature in the plots of σ_f versus log $\dot{\epsilon}$. A straigth line σ_f versus ln $\dot{\epsilon}$ relationship was therefore assumed and a least squares procedure gave the regularly space curves of Fig. 7. There was, however, an increse in the spacing of the σ_f versus log $\dot{\epsilon}$ plots with increasing strain. In terms of the Eyring representation this implies that the behaviour can be described by a single activated process at each level of strain, but the activation volume decreases with increasing strain, which is reasonable in physical terms.

The general form of the flow stress data is therefore

$$\sigma_f(\epsilon, \dot{\epsilon}) = \sigma_0(\epsilon) + k(\epsilon) \ln \dot{\epsilon} \quad (3)$$

If $k(\epsilon)$ were constant, corresponding to a constant activation volume, this would imply that strain hardening and strain rate effects were entirely separable, and Equation 3 would reduce to the expression proposed some time ago by Haward and Thackray for amorphous polymers [31]. The latter workers proposed that the behaviour of

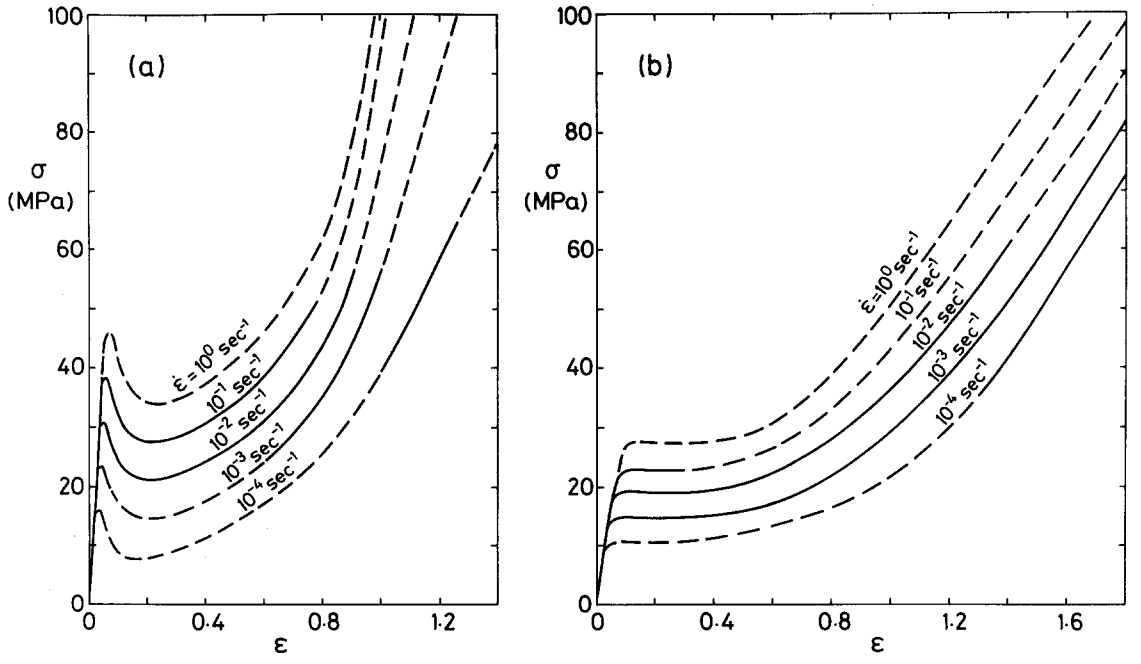

Figure 7 True stress–strain–strain rate relationships for PMMA at 90° C (a) Grade A (b) Grade B

these materials could be represented by a rubber elastic spring and an Eyring dashpot acting in parallel. The increase in $k(\epsilon)$ with increasing strain is small, suggesting that a modified version of the Haward and Thackray model may be of some use in the future. The broken curves in Fig. 7 represent values of σ_f obtained by extrapolation outside the experimental region of strain rates. Another interesting factor, apparent from Fig. 7, is that the higher molecular weight grade A exhibits substantial strain-softening, whereas grade B shows very little (both materials gave load maxima in the uncorrected test, the effect being more pronounced with the grade A samples). This can be attributed to the fact that the grade B material at 90° C is significantly closer to its T_g than grade A.

5.2. Effect of pressure

In our previous publications dealing with the mechanics of the hydrostatic extrusion behaviour of LPE and POM it was found convenient to use a Coulomb yield criterion [22, 23]. This was justified on the grounds that for most of the extrusion process we are dealing with a highly anisotropic material, in which we can envisage that deformation occurs by slip on chains containing the c-axis of the polymer. The effect of pressure on the flow stress can then be regarded as entering through the effect of the stress σ_y normal to the extrusion direction, which led to a flow criterion of the form

$$\sigma_x - \sigma_y = \sigma_f(\epsilon, \dot{\epsilon})(1 + \beta\sigma_y) \qquad (4)$$

where σ_x is the stress in the extrusion direction and β is a normal stress coefficient having the dimensions of inverse stress.

This form of the flow criterion produced a reasonable fit to data for LPE from room temperature tensile tests at various applied pressures [33], and fitted LPE and POM extrusion data very well indeed [22, 23].

For PMMA, however, the maximum degree of anisotropy is much lower than for LPE or POM, and so yield is more likely to be affected by the hydrostatic component of stress, σ_H, as is the case for isotropic materials. Rabinowitz *et al.* [34] observed that the yield stress of isotropic PMMA could be described by a relationship

$$\sigma = \sigma_o + \gamma\sigma_H \qquad (5)$$

in which γ is a dimensionless hydrostatic pressure coefficient. Assuming that use of the hydrostatic pressure effect is appropriate for extrusion of PMMA to give relatively low degrees of orientation, the resulting yield criterion becomes

$$\sigma_x - \sigma_y = \sigma_f(\epsilon, \dot{\epsilon}) + \gamma\sigma_H \qquad (6)$$

where the hydrostatic stress $\sigma_H = (\sigma_x/3) + (2\sigma_y/3)$.

The form of the yield criterion of Equation 6

may be argued from a natural extension of the Eyring equation [32] in which the strain rate is expressed as

$$\dot{\epsilon} = \dot{\epsilon}_o \exp - \left(\frac{\Delta U - \tau V + \sigma_H \Omega}{KT} \right) \quad (7)$$

where Ω is the pressure activation volume and τ is the shear yield stress. In terms similar to Equation 3, Equation 7 implies

$$\tau(\epsilon, \dot{\epsilon}) = \tau_o(\epsilon) + k(\epsilon) \ln \dot{\epsilon} + \gamma \sigma_H \quad (8)$$

where $\gamma = \Omega/V$ expresses the pressure dependence of the shear yield stress. Equation 8 can be appropriatley generalized to three dimensions by replacing τ by τ_{oct}, the octahedral stress. For our two dimensional problem we then have

$$\sigma_x - \sigma_y = \sigma_o(\epsilon) + k(\epsilon) \ln \dot{\epsilon} + \gamma \sigma_H \quad (9)$$

which is identical to Equation 6.

It should be noted that the flow criterion used for PMMA (Equation 6) differs from that used for LPE and POM (Equation 4) in the following two respects; (i) The effect of pressure is quantified by the hydrostatic, rather than the normal, component of stress. (ii) The pressure effect enters as an additive, rather than a multiplicative, term.

It has been verified that the additive, hydrostatic pressure effect produces a better fit to the experimental extrusion data for PMMA than the multiplicative, normal stress effect.

5.3. Mechanics of the extrusion process

The relationship between extrusion pressure and the plastic stress–strain curve has been widely examined for metals, where satisfactory analyses have been made in terms of either the Tresca or the Von Mises yield criterion. The effects of strain rate and pressure are usually sufficiently small to be neglected. By contrast, the plastic deformation behaviour of polymers cannot be treated so simply, as demonstrated in the analysis of Gibson, Coates and Ward [22, 23] for crystalline polymers. It was shown by this analysis that for LPE and POM both the strain rate and the pressure dependence of the material flow stress have marked effects on the extrusion pressure.

The analysis of the mechanics of the hydrostatic extrusion process for PMMA follows that of Gibson *et al.* almost exactly, but there are a number of important differences. These relate to the method of incorporating the pressure effect (discussed above) and to a method of equating the effects of pressure and friction (discussed in section 5.5). It can be seen from the work of Avitzur [18] that for small or moderate die angles deformation in a conical converging die occurs in a predominantly tensile manner, and so the true stress–strain–strain rate data derived from tensile tests may be used in an analysis of the process mechanics, provided (i) it is assumed that the characteristic true stress–strain–strain rate relationship is unique at a given temperature [27], and (ii) the strain and strain rate fields in the die are known.

The strain field may be specified in terms of the instantaneous deformation ratio R as

$$\epsilon = \ln R \quad (10)$$

Assuming a planar (plug flow) velocity profile, which does not satisfy continuity but is a good approximation at low die angles, the strain rate field may be given [22, 23] by

$$\dot{\epsilon} = \frac{4v_f}{d_f} \left(\frac{R}{R_N} \right)^{3/2} \tan \alpha \quad (11)$$

The treatment adopted here for plastic flow in a conical die is a modified form of Hoffman and Sachs' equation [17], which was originally derived for metals extrusion by considering the force balance on a thin, parallel sided element in the deformation zone, giving

$$\frac{d\sigma_x}{d\epsilon} = \sigma_x - \sigma_y(1 + L) \quad (12)$$

where $L = \mu \cot \alpha$, μ being the billet-die friction coefficient.

For the case of PMMA, the pressure dependent plastic flow criterion (Equation 6) can be used to eliminate σ_y from Equation 12, giving

$$\frac{d\sigma_x}{d\epsilon} = \sigma_x - (1 + L) \left[\frac{(1 - \gamma/3)\sigma_x - \sigma_f(\epsilon, \dot{\epsilon})}{(1 + 2\gamma/3)} \right] \quad (13)$$

In the absence of redundant work the above differential equation could be solved for the following boundary conditions;

$$\begin{aligned} &\text{(i) Die entrance; } \sigma_x = -P; \epsilon = 0 \\ &\text{(ii) Die exit; } \quad \sigma_x = 0; \quad \epsilon = \ln R_N \end{aligned} \quad (14)$$

It has been established, however, that redundant work is done (and additional strains imparted) at the entrance to and exit from the deformation zone, where the material flow is forced to change

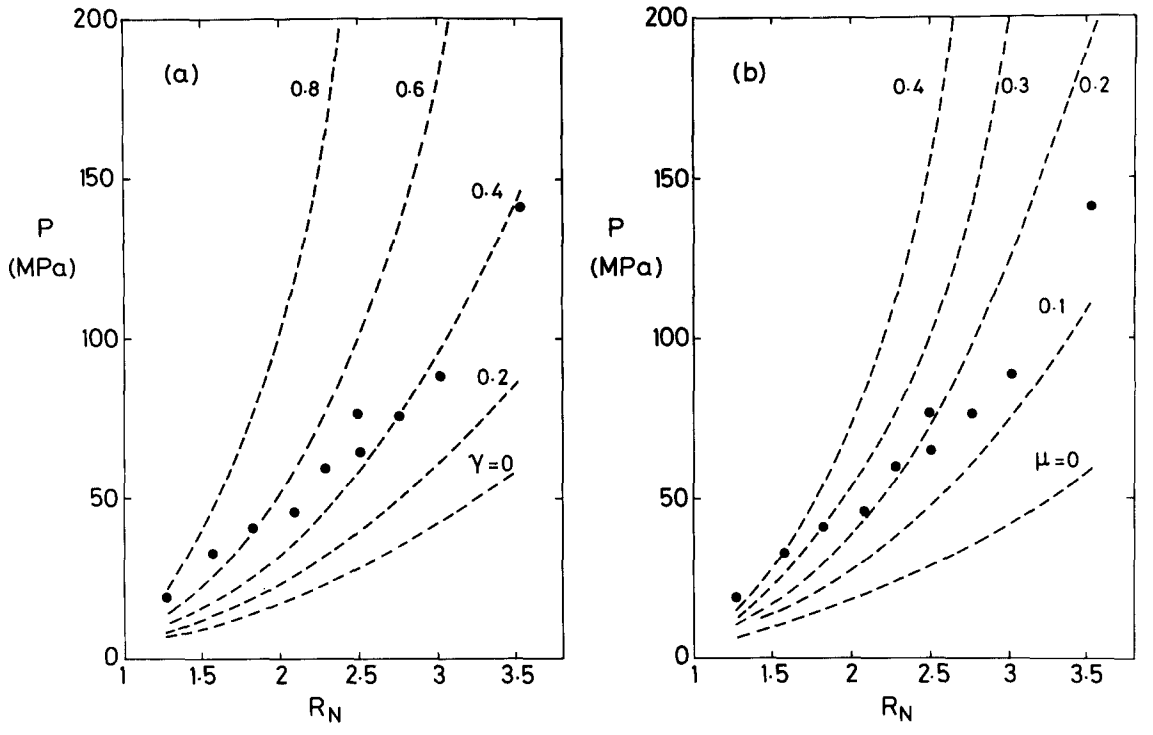

Figure 8 Comparison of experimental and computed extrusion pressures for Grade A at $T_N = 90°$ C ($v_f = 1$ mm min^{-1}) (a) Variation with γ ($\mu = 0$) (b) Variation with μ ($\gamma = 0$)

direction. The average redundant strain imparted at each of these boundaries is given [18, 25] (for spherical boundaries) by

$$\epsilon_{red} = \frac{1}{\sqrt{3}}\left(\frac{\alpha}{\sin^2 \alpha} - \cot \alpha\right) \quad (15)$$

The corresponding components of redundant work, P_1 and P_2, dissipated at the boundaries are given by

$$P_1 = \tau_1 \epsilon_{red} \quad \text{and} \quad P_2 = \tau_2 \epsilon_{red} \quad (16)$$

where τ_1 and τ_2 are the appropriate shear yield stresses of the material at the die entry and exit. Because of the pressure dependence of the yield stress (Equation 5), Equations 16 become

$$\begin{aligned} P_1 &= (\tau_1 + \gamma\sigma_H)\,\epsilon_{red} \\ P_2 &= (\tau_2 + \gamma\sigma_H)\,\epsilon_{red} \end{aligned} \quad (17)$$

Studies of the yield behaviour of oriented polymers show that the shear yield stress of the oriented polymer does not differ greatly from that of the isotropic polymer [34]. We have therefore assumed that the shear yield stress remains constant throughout the die and equal to the shear yield stress of the isotropic material (note that because the hydrostatic stress σ_H changes through the die, $P_1 \neq P_2$). This approximation has little effect on the final computed extrusion pressures, the main effect being to alter the strain boundary conditions, as follows;

$$\begin{aligned} &\text{(i)}\ \sigma_x = -P + P_1\,;\ \epsilon = \epsilon_{red} \\ &\text{(ii)}\ \sigma_x = -P_2 \quad ;\ \epsilon = \epsilon_{red} + \ln R_N \end{aligned} \quad (18)$$

Equation 13, which includes the effects of pressure, friction and the material stress–strain–strain rate behaviour, was solved numerically for the above boundary conditions to give the extrusion pressure for a given extrusion ratio, at a specified extrudate velocity and die-angle. The solution was performed using a computer program which involved three main stages: (i) computation of the strain and strain rate field in the deformation zone; (ii) calculation of the flow stress through the die, by interpolation from true stress–strain–strain rate data at the relevant values of strain and strain rate; (iii) numerical solution of the modified Hoffman and Sachs' equation (Equation 13) for the appropriate boundary conditions (Equation 14).

5.4. Comparison of computed and experimental extrusion pressures

Since the effects of pressure and friction are not separable in the present analysis (i.e. the factors γ and μ cannot be determined independently) computation was initially performed for the extreme cases of (a) zero friction ($\mu = 0$); variation

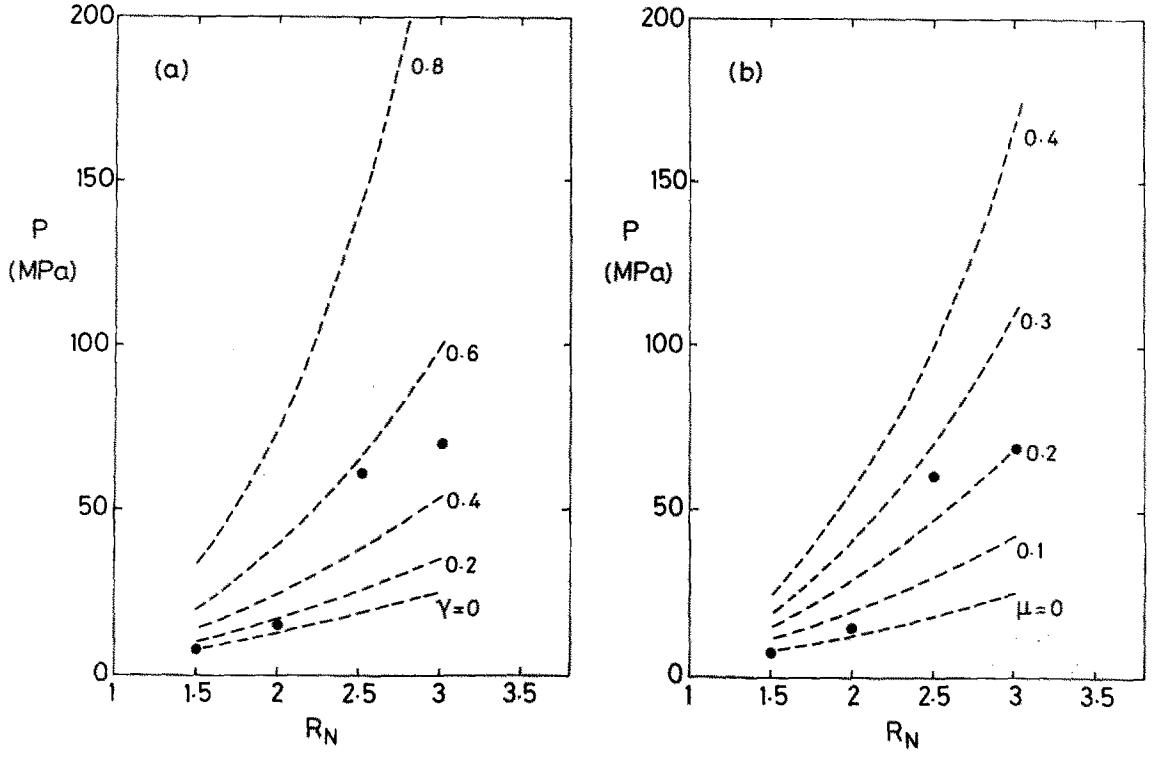

Figure 9 Comparison of experimental and computed extrusion pressures for Grade B at $T_N = 90°$ C ($v_f = 1$ mm min^{-1}) (a) Variation with γ ($\mu = 0$) (b) Variation with μ ($\gamma = 0$)

with γ (b) zero pressure dependence ($\gamma = 0$); variation with μ.

Figs. 8 and 9 show a comparison between the computed variation of extrusion pressure with extrusion ratio and the experimental results, for grades A and B respectively ($T_N = 90°$ C, $v_f = 1$ mm min^{-1}). An analysis was not performed for grade A at $T_N = 50°$ C because of the lack of true stress–strain–strain rate data at that temperature.

It can be seen from Figs. 8 and 9 that the major difference between the two grades is reproduced, although the detailed fits to the experimental data are not very good. The limited success of the detailed fitting is more likely due to the high scatter in experimental results rather than shortcomings in the analysis. This large scatter may be attributed either to the occurrence of "stick–slip", or to the possibility of deformational heating leading to non-isothermal extrusion conditions, both of which have been discussed. Nevertheless it is still possible and valid to consider the optimum values of the coefficients γ and μ predicted by the analysis.

Although it is not possible to distinguish whether the pressure-only or friction-only fits are bettter, evaluation by least squares fitting showed the optimum values of the coefficients (which of course represent upper bounds) to be in the region of $\gamma = 0.4$ and $\mu = 0.15$ for both grade A and grade B.

The emergence of similar values of γ and μ to given optimum fits for both molecular weight grades of PMMA suggests that the difference in extrusion pressures between the grades (Fig. 5) is indeed entirely a reflection of the difference in true stress–strain–strain rate behaviour (Fig. 7) and gives confirmation of the general approach which we have adopted.

Unlike metals extrustion, in which the relatively small degree of strain hardening causes the redundant work to be a significant proportion of the total extrusion pressure, the redundant work terms for PMMA are small. Although the value of redundant work ($P_1 + P_2$) increases slightly with extrusion ratio, the high strain hardening characteristics of the polymer, combined with the effects of pressure and strain rate, cause a rapid increase in extrusion pressure with extrusion ratio, and so redundant work represents less than 5% of the total work at $R_N = 3$, compared with typically 20 to 30% at very low extrusion ratios.

It should be noted that while the analysis includes the effect of strain rate and is valid at all extrusion rates, the results reported here (Figs. 8 and 9) are for a single extrudate velocity. No attempt was made to fit the variation of extrusion pressure with extrudate velocity to experimental data, largely because of the scatter of experimental results and the increased likelihood of non-isothermal extrusion at higher velocities.

5.5. Comparison of pressure and friction coefficients

The pressure and friction coefficients for PMMA extrusion are set in context in Table II, where they are compared with the results for LPE and POM obtained for hydrostatic extrusion [22, 23] and with static friction data from other sources [35, 36]. In order to obtain pressure coefficients for LPE and POM from the multiplicative type of normal stress coefficient used in references 22 and 23, it was necessary to multiply by the shear yield stress. Although the validity of such a simple procedure may appear to be questionable, it will be seen later that differences between the normal stress and the hydrostatic component of stress may be neglected for our present purposes. A much larger pressure effect is indicated for PMMA than for the crystalline polymers, which is physically reasonable.

The friction coefficient of PMMA obtained in hydrostatic extrusion is also much larger than that of LPE or POM, which could account for the incidence of marked "stick–slip" behaviour observed in PMMA extrusions.

While the upper-bound friction coefficients for hydrostatic extrusion follow the same trend as the static coefficients obtained in sliding tests on unlubricated steel, the values are very much lower. The values for PMMA extrusion are, however, greater than those obtained in the hydrostatic extrusion of metals, where hydrodynamic lubrication is known to occur. Although a film of extrusion fluid becomes entrained between the billet and the die during the extrusion of PMMA, the higher friction coefficients indicate that asperity contact must occur between the polymer and the die, that is to say extrusion occurs under conditions of boundary lubrication.

From Table II a correlation between the upper bounds of the friction and pressure coefficients is clearly indicated for the hydrostatic extrusion of different polymers. Such a correlation has been

TABLE II Comparison of pressures and friction coefficients for PMMA, LPE and POM.

Material	Upper bounds obtained from analysis of hydrostatic extrusion process		Coefficient of static friction in contact with steel
	γ	μ	
PMMA	0.4	0.15	0.4–0.5
LPE	0.01–0.02	0.03	0.2
POM	0.02–0.05	0.075	0.15–0.35

observed recently by Briscoe and Tabor [37, 38], while comparing the shear properties of thin polymer films to their coefficients of friction. In sliding tests on polymer films the shear strength τ was found to be related to the contact stress σ_p by a relationship similar in form to Equation 5, namely

$$\tau = \tau_o + \gamma' \sigma_p \tag{19}$$

where γ' is a stress coefficient. Consideration of the frictional force arising as a result of a shearing process within (or at the surface of) the polymer leads to an adhesive coefficient of friction given by

$$\mu = \frac{\tau_o}{\sigma_p} + \gamma' \tag{20}$$

It has been remarked [39] that in the case of a thin polymer film sliding between two surfaces the hydrostatic component of stress σ_H can be considered to be in the region of 95% of the normal contact stress σ_p. If σ_p is replaced in Equation 20 by σ_H, then γ' may be replaced by γ, giving

$$\mu = \frac{\tau_o}{\sigma_H} + \gamma \tag{21}$$

In the case of thin polymer films the shear stress at zero pressure (τ_o) is very much lower than the bulk value for the polymer. If we assume that this is also the case during hydrostatic extrusion, then the first term in Equation 21 becomes small compared to the second, and so

$$\mu \simeq \gamma \tag{22}$$

Introduction of the equivalence of μ and γ into the analysis of the process mechanics allows the computed extrusion pressures to be fitted to the experimental data by the use of a single parameter $\mu(=\gamma)$, and allows an optimum value to be determined uniquely for each material (thereby obviating the upper bound approach of section 5.4 and references 22 and 23). This has been done in Fig. 10, from which it can be seen that the most

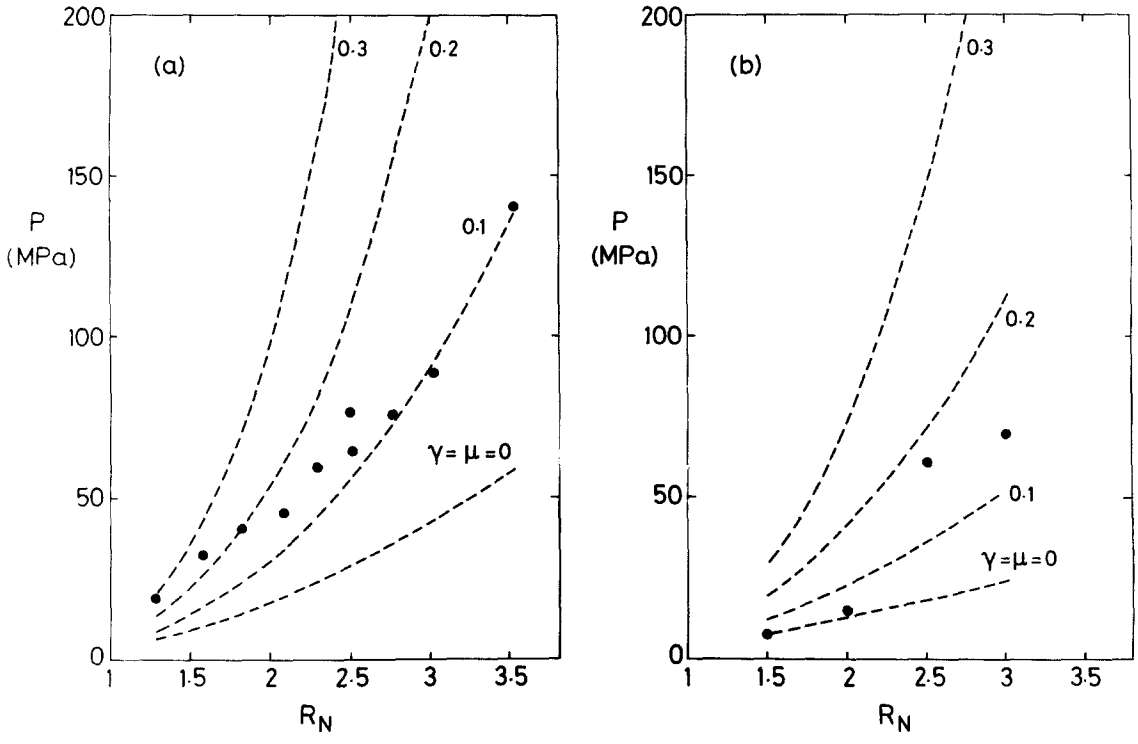

Figure 10 Comparison of experimental and computed extrusion pressures at $T_N = 90°$ C for $\mu = \gamma$ (a) Grade A (b) Grade B

reasonable fits to the experimentally observed pressures are obtained for $\mu(=\gamma)$ in the range 0.1 to 0.2. As a pressure coefficient $\gamma \sim 0.1$ to 0.2 compares very well with those obtained previously for PMMA at 25° C ($\gamma = 0.204$ in torsion under hydrostatic pressure [34]; 0.175 from data in plane strain compression [40]). As a friction coefficient $\mu \sim 0.1$ to 0.2 is still much less than the static coefficient of friction against steel, but considerably higher than the values obtained in the hydrostatic extrusion of crystalline polymers.

6. Conclusions

The hydrostatic extrusion of PMMA is limited to much lower degrees of deformation than are possible in crystalline polymers. This is mainly a result of the brittle nature of the material, and reflects the lower degrees of deformation which are obtained in the tensile drawing of PMMA, but is also due partly to the increased effects of friction and pressure on the material flow stress.

The occurence of the phenomenon of "stick–slip" was evident in all extrusions, and is a consequence of the high friction between the billet and the extrusion die. This resulted in a larger scatter of extrusion pressures than had been observed previously for crystalline polymers, with a greater sensitivity to the surface condition of the extrusion billets.

As in the case of crystalline polymers, it proved necessary to take into account the effects of strain headening, strain rate and pressure dependence of the flow stress when analysing the mechanics of the extrusion process. By analogy with the friction behaviour of thin polymer films it is possible to consider the effect of friction in the process as equivalent to that of pressure, allowing the process mechanics model to be fitted to the extrusion data by varying a single parameter.

The true stress–strain–strain rate behaviours of the two grades of PMMA investigated were found to be markedly different, and a correlation with T_g is indicated. These differences in flow stress were reflected directly by the observed extrusion pressures, supporting the assumption of a unique tensile true stress–strain–strain rate relationship for a given temperature.

References

1. A. BUCKLEY and H. A. LONG, *Polymer. Eng. Sci.* 9 (1969) 115.
2. K. IMADA, T. YAMAMOTO, K. SHIGEMATSU and M. TAKAYANAGI, *J. Mater. Sci.* 6 (1971) 537.
3. T. WILLIAMS, *ibid.* 8 (1973) 59.
4. A. G. GIBSON, I. M. WARD, B. N. COLE and B.

PARSONS, *ibid.* 9 (1974) 1193.
5. A. G. KOLBECK and D. R. UHLMANN, *J. Polymer Sci. Polymer Phys. Ed.* **15** (1977) 27.
6. A. G. GIBSON and I. M. WARD, *ibid.* **16** (1978) 2015.
7. P. D. COATES and I. M. WARD, *ibid.* **16** (1978) 2031.
8. P. S. HOPE, A. G. GIBSON, B. PARSONS and I. M. WARD, *Polymer Eng. Sci.* in press.
9. P. S. HOPE and B. PARSONS, *ibid.* in press.
10. P. S. HOPE, A. G. GIBSON and I. M. WARD, *J. Polymer Sci., Polymer Phys. Ed.* in press.
11. S. ABDUL JAWAD and I. M. WARD, *J. Mater. Sci.* **13** (1978) 1381.
12. A. G. GIBSON, D. GREIG, M. SAHOTA, I. M. WARD and C. L. CHOY, *J. Polymer Sci. Polymer Lett. Ed.* **15** (1977) 183.
13. J. M. ALEXANDER and P. J. H. WORMELL, *Ann. C.I.R.P.* **19** (1971) 21.
14. K. D. PYE, S. K. BHATEGA and J. A. SAUER, Proceedings of the NEL/AIRAPT International Conference on Hydrostatic Extrusion (NEL, Glasgow, 1973).
15. N. KAHAR, R. A. DUCKETT and I. M. WARD, *Polymer* **19** (1978) 136.
16. P. S. HOPE, A. G. GIBSON and I. M. WARD, unpublished work.
17. O. HOFFMAN and G. SACHS, "Introduction to the Theory of Plasticity for Engineers" (McGraw-Hill, New York, 1953).
18. B. AVITZUR, "Metal Forming: Processes and Analysis" (McGraw-Hill, New York, 1968).
19. S. MARYAMA, K. IMADA and M. TAKAYANAGI, *International J. Polymeric Mater.* **1** (1972) 211.
20. *Idem, ibid.* **2** (1973) 105.
21. *Idem, ibid.* **2** (1973) 125.
22. A. G. GIBSON, P. D. COATES and I. M. WARD, "Science and Technology of Polymer Processing" Edited by N. P. Suh and N. H. Sung, (M.I.T. Press, Massachusetts 1979).
23. P. D. COATES, A. G. GIBSON and I. M. WARD, *J. Mater. Sci.* **15** (1980) 359.
24. P. S. HOPE, R. A. DUCKETT and I. M. WARD, *J. Appl. Polymer Sci.*, in press.
25. H. LI. D. PUGH, "Mechanical Behaviour of Materials under Pressure", (Elsevier, Amsterdam, 1970).
26. J. S. HARRIS, I. M. WARD and J. S. C. PARRY, *J. Mater. Sci.* **6** (1971) 110.
27. P. D. COATES and I. M. WARD, *J. Mater. Sci.* **13** (1978) 1957.
28. P. I. VINCENT, *Polymer* **1** (1967) 7.
29. A. S. ARGON, in "The Inhomogeneity of Plastic Deformation", (A.S.M. Metals Park Ohio, 1973) ch. 7.
30. C. BAUWENS-CROWET, *J. Mater. Sci.* 8 (1973) 968,
31. R. N. HAWARD and G. THACKRAY, *Proc. Roy. Soc.* **A302** (1968) 453.
32. I. M. WARD, *J. Mater. Sci.* **6** (1971) 1397.
33. L. A. DAVIS and C. A. PAMPILLO, *J. Appl. Phys.* **42** (1971) 4659.
34. S. RABINOWITZ, I. M. WARD and J. S. C. PARRY, *J. Mater. Sci.* **5** (1970) 29.
35. "Handbook of Chemistry and Physics" Edited by R. C. Weast (Chemical Rubber Publishing Co., Cleveland, 1973).
36. Manufacturers data.
37. B. J. BRISCOE and D. TABOR, in "Polymer Surfaces" Edited by D. T. Clark and W. J. Feast (Wiley-Interscience, New York, 1978) ch. 1.
38. *Idem, J. Adhesion* **9** (1978) 145.
39. B. J. BRISCOE, private communication.
40. P. B. BOWDEN and J. A. JUKES, *J. Mater. Sci.* **3** (1968) 183.

Received 17 January and accepted 30 January 1980.

Note: since the paper was accepted for publication the authors have found Equations 7 and 8 to contain an inconsistency, in that the pressure coefficient appropriate to shear deformation differs from that for tensile deformation by a factor which approximates numerically to 2. As a result the pressure coefficient relating to tensile flow stress data is related to the friction coefficient by the relationship $\gamma \triangleq 2\mu$, and this should have been used rather than Equation 22, which relates to shear. The extrusion pressures have been re-computed and were found to fit the experimental data equally well, the only difference being that slightly lower friction coefficients are predicted for optimum fits (μ of the order of ~ 0.1 for both grades of PMMA).